Biochimica et Biophysica Acta 1838 (2014) 173–184

Contents lists available at ScienceDirect

Biochimica et Biophysica Acta

journal homepage: www.elsevier.com/locate/bbamem

Interaction of prenylated chalcones and flavanones from common hop with phosphatidylcholine model membranes

Olga Wesołowska [a,*,1], Justyna Gąsiorowska [a,1], Joanna Petrus [b], Bogusława Czarnik-Matusewicz [b], Krystyna Michalak [a]

[a] Department of Biophysics, Wroclaw Medical University, ul. Chalubinskiego 10, 50-368 Wroclaw, Poland
[b] Faculty of Chemistry, University of Wroclaw, ul. Joliot-Curie 14, 50-383 Wroclaw, Poland

ARTICLE INFO

Article history:
Received 15 May 2013
Received in revised form 20 August 2013
Accepted 13 September 2013
Available online 21 September 2013

Keywords:
DPPC model membranes
8-Prenylnaringenin
Xanthohumol
Isoxanthohumol
Microcalorimetry (DSC)
ATR-FTIR

ABSTRACT

Common hop (*Humulus lupulus*) constitutes a source of numerous prenylated chalcones such as xanthohumol (XH) and flavanones such as 8-prenylnaringenin (8-PN) and isoxanthohumol (IXH). Range of their biological activities includes estrogenic, anti-inflammatory, anti-infective, anti-cancer, and antioxidant activities. The aim of the present work was to characterize the influence of prenylated polyphenols on model 1,2-dipalmitoyl-*sn*-glycero-3-phosphocholine (DPPC) membranes by means of differential scanning calorimetry (DSC), fluorescence and attenuated total reflection Fourier transform infrared (ATR-FTIR) spectroscopies. All studied compounds intercalated into DPPC bilayers and decreased its melting temperature as recorded by DSC, Laurdan and Prodan fluorescence, and ATR-FTIR. Polyphenols interacted mainly with glycerol backbone and acyl chain region of membrane. Magnitude of the induced effect correlated both with lipophilicity and molecular shape of the studied compounds. Elbow-shaped 8-PN and IXH were locked at polar–apolar region with their prenyl chains penetrating into hydrophobic part of the bilayer, while relatively planar XH molecule adopted linear shape that resulted in its deeper insertion into hydrophobic region. Additionally, by means of DSC and Laurdan fluorescence IXH was demonstrated to induce lateral phase separation in DPPC bilayers in gel-like state. It was assumed that IXH-rich and IXH-poor microdomains appeared within membrane. Present work constitutes the first experimental report describing interactions of prenylated hop polyphenols with phospholipid model membranes.

1. Introduction

Common hop (*Humulus lupulus*) constitutes a source of numerous prenylated chalcones such as xanthohumol (2′,4′,4-trihydroxy-6′-methoxy-3′-prenylchalcone; XH) and flavanones such as 8-prenylnaringenin (8-PN) and its 5-O-methyl derivative, isoxanthohumol (IXH) (for chemical structures see Fig. 1). The total daily intake of hop prenylflavonoids may reach 0.14 mg, and their main source in human diet is beer since hop female flowers are used as flavoring agent and preservative in production of this beverage [1]. The range of recognized biological activities of these compounds is very wide. 8-PN, apart from being a potent phytoestrogen [2], has been also found to be an inhibitor of aromatase, a key enzyme in estrogen biosynthesis [3]. Inhibitory activities of XH and IXH in this respect were much weaker. Additionally, 8-PN can inhibit angiogenesis [4] and act as a vascular-protective agent [5,6]. All three compounds have been reported to possess anti-inflammatory activity [5,7], XH has also been identified as an anti-infective agent [8]. Prenylated flavonoids from hops have been found to inhibit proliferation of lung, ovarian, melanoma, and colon cancer cells [9] as well as breast [10,11] and prostate cancer cells [12]. Additionally, XH induced apoptosis in prostate cancer [13,14] and in acute lymphocytic leukemia cells [15]. Moreover, XH and 8-PN have been observed to modulate expression [9] and activity [16] of transporters associated with multidrug resistance of cancer cells. Prenylated hop flavonoids, especially XH, possess also a significant antioxidant activity and are able to inhibit LDL [17,18] and liver microsomal lipid peroxidation [19].

The aim of the present work was to characterize the influence of main prenylated chalcone and flavanones from hops on model lipid membranes formed from phosphatidylcholine. Until now, the interaction of 8-PN, XH and IXH with lipid bilayers has been hardly studied. According to our best knowledge, only one report exists notifying

Abbreviations: ATR-FTIR, attenuated total reflection Fourier transform infrared spectroscopy; DMPC, 1,2-dimyristoyl-*sn*-glycero-3-phosphocholine; DPPC, 1,2-dipalmitoyl-*sn*-glycero-3-phosphocholine; DSC, differential scanning calorimetry; ΔH, transition enthalpy; GP, generalized polarization; IXH, isoxanthohumol; λ_{ex}, excitation wavelength; PCA, principal component analysis; PC1, first principal component; 8-PN, 8-prenylnaringenin; $T_{1/2}$, calorimetric peak half-height width determined from thermograms; ΔT_M^{IR}, width of the transition determined from infrared spectra; T_M, main phase transition temperature determined from thermograms; T_M^{IR}, main phase transition temperature determined from infrared spectra; XH, xanthohumol

* Corresponding author at: Department of Biophysics, Wrocław Medical University, Chalubinskiego 10, 50-368 Wroclaw, Poland. Tel.: +48 71 8741415; fax: +48 71 7848800.
E-mail address: olga.wesolowska@umed.wroc.pl (O. Wesołowska).

[1] These authors contributed equally to this work.

0005-2736/$ – see front matter © 2013 Elsevier B.V. All rights reserved.
http://dx.doi.org/10.1016/j.bbamem.2013.09.009

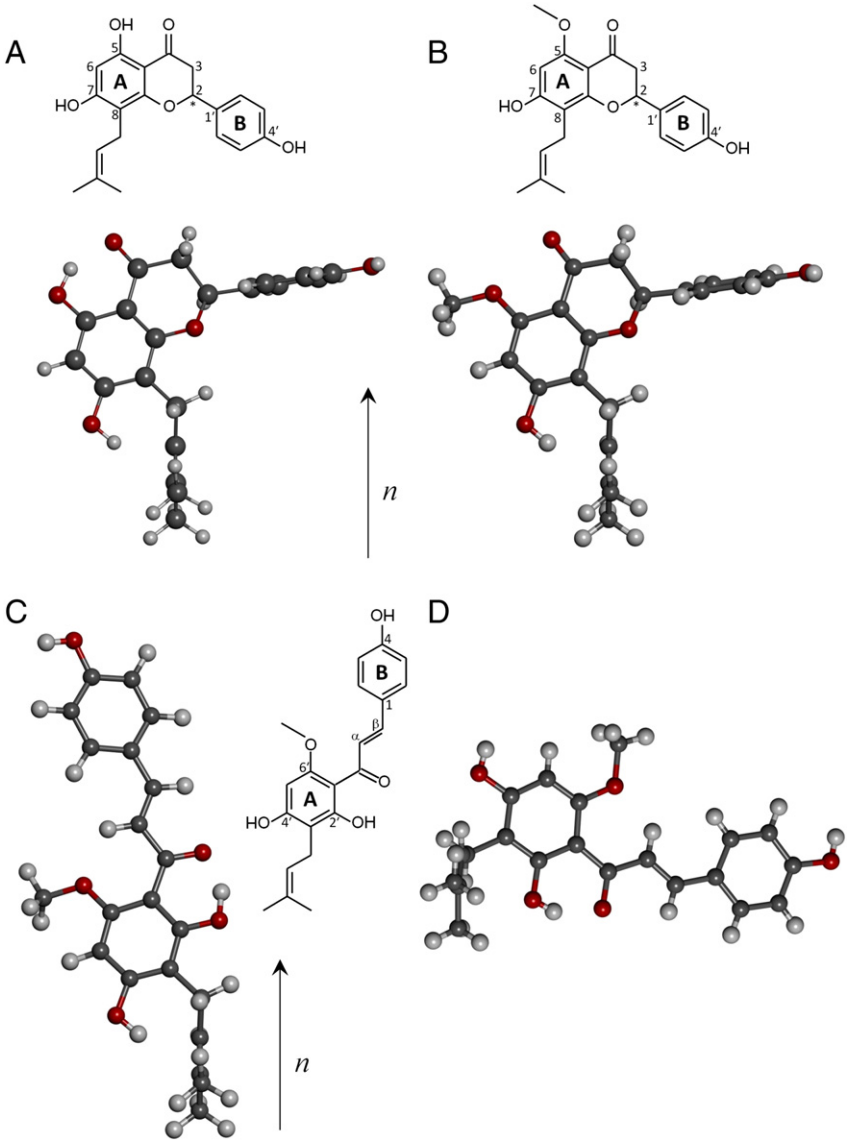

Fig. 1. The 2D presentations and the ball and stick presentations of the optimized structures for 8-PN (A), IXH (B), XH (C) and structure of XH according to the X-ray results [23] (D). The molecules have common orientation of the prenyl chain, i.e. parallel to the bilayer normal (*n*). For racemic 8-PN and IXH the chiral C2 atoms are marked by * on the 2D presentation, their 3D presentations correspond to the 2S(−) enantiomers.

interaction of XH with model lipid systems [20], and virtually none for 8-PN and IXH. Arczewska et al. [20] have used X-ray diffraction and FTIR spectroscopy to characterize the interaction of XH with dry DPPC multibilayers. The obtained results allowed the authors to conclude that XH affected molecular organization and structural properties of the polar part of the bilayer. In the present work we have employed differential scanning calorimetry (DSC), fluorescence spectroscopy and attenuated total reflection Fourier transform infrared spectroscopy (ATR-FTIR) to characterize the interaction of three main prenylated hop flavonoids: 8-PN, XH and IXH with fully hydrated phospatidylcholine membranes. We have shown that all of the studied compounds intercalated into lipid bilayer and affected its biophysical properties. The polyphenols interacted mainly with glycerol backbone and acyl chain region of the membrane. The magnitude of the induced effect was correlated both with the lipophilicity and the molecular shape of these compounds. Additionally, IXH was demonstrated to induce lateral lipid phase separation in phosphatidylcholine bilayers. According to our best knowledge, the present work constitutes the first experimental report aiming to characterize the interactions of main prenylated hop polyphenols with phospholipid model membranes.

2. Materials and methods

2.1. Materials

Racemic mixtures of prenylated flavanones: 8-prenylnaringenin (8-isopentenylnaringenin), isoxanthohumol (5-O-methyl-8-prenylnaringenin) and its chalcone analog, xanthohumol were purchased from Alexis Biochemicals (Lausen, Switzerland). DPPC (1,2-dipalmitoyl-*sn*-glycero-3-phosphatidylcholine; L-α-dipalmitoylphosphatidylcholine) and DMPC (1,2-dimyristoyl-*sn*-glycero-3-phosphatidylcholine; L-α-dimyristoyl-phosphatidylcholine) were purchased from Avanti Polar Lipids (Alabaster, AL, USA). Laurdan (2-(dimethylamino)-6-dodecanoylnaphthalene) and Prodan (2-(dimethylamino)-6-propionylnaphthalene) were from Molecular Probes (Eugene, OR, USA).

Lipids were used without further purification and all other chemicals were of analytical grade.

2.2. Differential scanning calorimetry (DSC)

Polyphenol stock solutions were prepared in methanol (final concentration of 3.5 mM). 2 mg of phospholipid was dissolved in appropriate amount of polyphenol stock solution in order to obtain the desired drug:lipid molar ratio. The samples were then dried under the stream of nitrogen and placed under vacuum for at least 2 h. Next, 15 μl of 20 mM Tris–HCl buffer (150 mM NaCl, 0.5 mM EDTA, pH 7.4) was added to each sample. Mixture were heated to a temperature about 10 °C higher than the gel–liquid crystalline phase transition temperature and shaken in a thermostated mechanical shaker for several minutes. When homogeneity was obtained samples were sealed in aluminum pans.

Calorimetric measurements were performed using DSC 600 microcalorimeter (UNIPAN, Warsaw, Poland) at scan rate 1 °C/min. Samples were scanned immediately after preparation. At least 2 samples were prepared for each polyphenol:lipid molar ratio and each sample was measured at least 4 times. Calorimetric data were analyzed off-line using software developed in our laboratory.

2.3. Fluorescence spectroscopy

Small unilamellar liposomes, prepared by sonication of 2 mM DPPC suspension in 20 mM Tris–HCl buffer (0.1 mM EDTA, 50 mM NaCl, pH 7.4) using UP 200s sonicator (Dr Hilscher GmBH, Berlin, Germany), were used for fluorescence spectroscopy measurements. Final phospholipid concentration in a sample was 200 μM. Laurdan and Prodan were dissolved in DMSO in order to obtain 1 mM stock solutions. Liposomes were incubated with a fluorescent probe (final concentration 5 μM) for 15 min in darkness at room temperature. Then the appropriate amount of polyphenol stock solution (5 mM in DMSO) was added and the sample was further incubated for 30 min in darkness.

Steady-state fluorescence emission spectra were recorded by LS 50B spectrofluorimeter (Perkin-Elmer Ltd., Beaconsfield, UK) equipped with a xenon lamp with excitation and emission slits set to 5 nm. The temperature in a cuvette containing magnetic stir bar was measured by platinum thermometer and maintained under control of water circulating bath. Fluorescence intensity dependence on temperature was recorded at excitation wavelengths 390 nm and 380 nm for Laurdan and Prodan, respectively. Recorded fluorescence spectra were processed with FLDM Perkin-Elmer 2000 software.

The generalized polarization (GP) was calculated according to the equation provided by Parasassi et al. [21]:

$$GP = \frac{I_B - I_R}{I_B + I_R} \quad (1)$$

where I_R and I_B are the fluorescence emission intensities at the blue and red edges of the emission spectrum, respectively. For both fluorescence probes I_B was measured at 440 nm, while I_R was recorded at 490 nm for Laurdan and 480 nm for Prodan. It was checked that the studied polyphenols alone did not exhibit fluorescence in the spectral region of interest. All experiments were performed in triplicate.

2.4. ATR-FTIR (attenuated total reflection Fourier transform infrared) spectroscopy

Polyphenol stock solutions (final concentration 1 mM) were prepared in chloroform or in chloroform:methanol (1:1) in case of IXH. For each sample 10 mg of DPPC was dissolved in an appropriate amount of the solution to obtain polyphenol:DPPC molar ratio equal to 0.06. The solution was dried and placed under vacuum for at least 20 min. The dry flavonoid:DPPC film was hydrated by 1 ml of double distilled water (Millipore, Milli Q) at 55 °C. Next, the liposome suspensions were treated by 5 times repeated thermal cycling (10 min at 4 °C, then 10 min at 55 °C) and at the end calibrated by 20-fold extrusion through 100 nm Nuclepore polycarbonate filter (Whatman). Finally, liposomes were spread on the surface of resistively heated ZnSe ATR crystal plate (face angle: 45°; 10 reflections, Pike Technologies, Inc., USA). The ATR-FTIR spectra were recorded with a Nicolet Avatar 360 FTIR spectrometer. For each spectrum 64 scans were collected with a spectral resolution of 1 cm^{-1} in the spectral region from 4000 cm^{-1} to 400 cm^{-1}. The spectra of the liposome suspensions and independently of the double distilled water were recorded in a heating cycle from 27 to 66 °C. Before spectrum acquisition, the liposomal suspension or water was equilibrated for 5 min at a given temperature.

2.5. ATR-FTIR data pretreatment and principal component analysis (PCA)

The infrared studies were performed for polyphenol:lipid molar ratio of 0.06 for each system because according to DSC results, the compounds affected model membrane properties most significantly starting from this value of molar ratio.

First, the ATR-FTIR spectrum of water was subtracted from spectrum of liposome sample measured at the same temperature. The spectral region around 2125 cm^{-1} is well suited to check for the correct subtraction of liquid water because this region is usually composed only from water bands and is free from lipid absorbance. The absorbance from analyzed compounds was negligible in this region, too. Generally, a complete subtraction of the water bands is not possible because water bound to lipids may exhibit altered band shapes. However, here it was possible to obtain the decay of the absorbance around 2125 cm^{-1} to zero for the subtracted spectra. Moreover, after subtraction the absorbance of the high and low frequency wings of the analyzed bands from lipids dropped to the same level close to zero.

Obtained difference spectra were used in further analysis, i.e. for each polyphenol they were arranged into individual data matrices. Then, they were offset corrected at 3800 cm^{-1} in order to reduce the baseline fluctuation between spectra. Afterward, two regions from 3000 cm^{-1} to 2800 cm^{-1} and from 1790 cm^{-1} to 1690 cm^{-1} were extracted for further analysis. Both spectral regions were baseline corrected by a linear function based on two limited points. In a next step the data matrices from the two regions were subjected to a smoothing procedure by the Savitzky–Golay algorithm. All the above pretreatment procedures were done using the Grams/32 Software (Galactic Industries from Thermo Scientific). Finally, the data matrices (individual for each sample) were transferred to Matlab (The MathWorks, Inc., Natick, MA, USA) for final calculations. The absorbance changes in both regions were analyzed independently by means of principal component analysis (PCA) for each polyphenol. Before the PCA was started the standard normal variate (SNV) pretreatment was applied to remove the component of absorbance controlled by the non-specific effects. The PCA has been performed using the PLS Toolbox for Matlab (Eigenvector Research, Inc.). Spectral variations captured by the first principal component (PC1) were taken for further analysis as this component models the changes strictly correlated with the temperature-induced transition. The scores values for PC1 against temperature (T) in Celsius degree were fitted by sigmoidal function:

$$\text{Scores}(T) = \frac{a_1 - a_2}{1 + \exp\left((T - T_M^{IR})/\Delta T_M^{IR}\right)} + a_2. \quad (2)$$

The main transition temperature, T_M^{IR}, and parameter ΔT_M^{IR} describing width of the transition that corresponds to a measure of cooperativity of the transition from gel to liquid crystalline phase were determined from the infrared spectra. The a_1 and a_2 are two additional parameters related to limited scores values at lower and higher temperatures, respectively.

2.6. Theoretical calculations

The geometries of isolated polyphenols were fully optimized in the gaseous phase by the density functional three-parameter model (B3LYP) using the 6-311++G(d,p) basis set with Gaussian 09 package [22]. Several initial structures for each polyphenol were considered. In case of XH the starting conformation was taken from the X-ray results [23] deposited in the Cambridge Structural Database (the CSD refcode: FARQOF) [24].

The 1-octanol/water partition coefficients (logP) were calculated by means of the ALOGPS program which utilizes several parallel algorithms to obtain logP value. The results are given as an average of all calculations ± standard deviation. A more detailed description of the ALOGPS 2.1 can be found elsewhere [25]. The applet that provides interactive on-line prediction of logP using the ALOGPS 2.1 is accessible through a website of Virtual Computational Chemistry Laboratory (VCCLAB, http://www.vcclab.org).

3. Results

3.1. Theoretical calculations

In the search for the most stable conformers, different orientations of the hydroxyl and methoxyl groups, and the prenyl unit in respect to the flavonoid skeleton were examined for all three compounds. In case of 8-PN and IXH the energy scans were also done for different relative orientations between the two phenyl rings A and B from the flavonoid unit. In XH the chalcone unit tends to be planar, as shown in the X-ray structure, due to the π-electron conjugation.

The structures presented in Fig. 1 and discussed below are fully geometry-optimized isolated monomers which stability was checked by positive vibrational frequencies. Compounds in Fig. 1 are oriented in such a fashion that the long axis of the prenyl unit and the membrane normal (*n*) are parallel. The optimized 3D structures for 8-PN and IXH correspond to the 2S(−) enantiomers.

The calculation of logP values identified XH as the most lipophilic compound of the set (4.38 ± 0.78), followed by IXH (3.82 ± 0.86) and 8-PN (1.39 ± 0.46).

3.2. Microcalorimetry

Differential scanning calorimetry has been employed to investigate the influence of the studied polyphenols on thermotropic properties of DPPC model membranes. The exemplary thermograms of DPPC recorded in the presence of increasing amounts of 8-PN, XH and IXH are presented in Fig. 2A, B and C, respectively. In pure DPPC two phase transitions were recorded, pretransition and main phase transition. The addition of any of the studied compounds resulted in vanishing of the pretransition. Polyphenols caused also the lowering of the temperature of main phase transition and the broadening of calorimetric peaks. Both effects increased with the increase of polyphenol:DPPC molar ratio. In case of XH, main phase transition was almost completely abolished at XH:DPPC molar ratio 0.12. In thermograms obtained for IXH (Fig. 2C), the asymmetry of the transition peaks was noticed starting from IXH:DPPC molar ratio 0.06. Low temperature shoulders of the peaks became longer than high temperature ones. Additionally, at IXH:DPPC molar ratios 0.08 and 0.12 the peaks appeared to be composed of two overlapping peaks.

All the studied compounds caused the concentration-dependent decrease of main phase transition temperature T_M (Fig. 3A) and the increase of peaks' half-height width $T_{1/2}$ (Fig. 3C). The comparison of the effects exerted by the studied polyphenols at molar ratio 0.12 on these two parameters revealed that the strongest model membrane perturbant was XH, IXH acted more weakly, while 8-PN exerted the most subtle effect. On the other hand, the influence of the studied compounds on transition enthalpy (Fig. 3B) was very weak, only XH caused noticeable enthalpy decrease.

Since the effect of polycyclic compounds on lipid thermotropic properties are usually more pronounced in phospholipids possessing shorter acyl chains [26,27], DMPC, the phospatidylcholine species with acyl chains two carbon atoms shorter than DPPC, was used to fully characterize the effect of the studied polyphenols on phosphatidylcholine model membranes. Fig. 2 shows the thermograms of DMPC membranes doped with 8-PN (Fig. 2D), XH (Fig. 2E) and IXH (Fig. 2F). Again, for pure DMPC both pretransition and main phospholipid phase transition were observed. Apart from vanishing of the pretransition, the decrease of T_M together with calorimetric peak broadening was observed in the presence of the studied polyphenols. Generally, the short-chain lipid was affected more strongly than the long-chain one. XH caused almost complete vanishing of main phospholipid transition at XH:DMPC molar ratio 0.06, and 8-prenylnaringenin caused such an effect at 8-PN:DMPC molar ratio 0.08. In case of IXH, significant asymmetry of peaks was noticed for IXH:DMPC molar ratios in the range 0.04–0.08, while for the ratios 0.10 and 0.12 an additional peak appeared in the temperature lower than the original peak (Fig. 2F).

Similarly, as in DPPC also in DMPC all studied compounds reduced T_M (Fig. 3D) and increased $T_{1/2}$ in a concentration-dependent manner (Fig. 3F). The comparison of the effects exerted on $T_{1/2}$ at polyphenol:DMPC molar ratio 0.06 (the highest molar ratio studied for all compounds) resulted in an order XH > IXH > 8-PN. Transition enthalpy of DMPC was changed by the studied polyphenols to a greater extent than in DPPC (Fig. 3E). All studied compounds exerted a biphasic effect on this parameter — transition enthalpy was increased in low polyphenol:DMPC molar ratios and reduced in higher molar ratios.

3.3. Fluorescence spectroscopy

Two fluorescent probes, Prodan and Laurdan, were employed to characterize the interaction of the studied polyphenols with DPPC liposomes. Both probes possess the same fluorophore but connected to the propionyl chain in case of Prodan and to the lauryl chain in Laurdan [28]. Laurdan fluorophore is located at the level of the phospholipid glycerol backbone, and Prodan, in contrast, is anchored to the lipid bilayer more loosely and resides closer to the membrane surface. In our studies first it was checked if the addition of any of the studied compounds would result in fluorescence quenching of the probes. Stern–Volmer plots are presented in Fig. 4A for XH and Fig. 4B for IXH and 8-PN. XH caused very strong quenching of both probes, the effect was, however, much more pronounced in case of Prodan. On the other hand, only very limited quenching of Prodan fluorescence was observed for IXH and 8-PN, while none of the two compounds had any impact on Laurdan fluorescence intensity (data not shown). Because of strong fluorescence quenching caused by XH all further fluorescence spectroscopy experiments were performed only for IXH and 8-PN.

Spectral properties of both Laurdan and Prodan depend strongly on bilayer phase state. In liquid-crystalline state the emission maximum of both probes is c.a. 50 nm red-shifted in comparison to the maximum in gel state (see Supplementary data, Fig. S1 for original fluorescence spectra recorded in different temperatures). Therefore, monitoring Laurdan or Prodan generalized polarization (GP) as a function of temperature constitutes a useful tool for monitoring thermotropic properties of model membranes. When phospholipid phase transition was monitored by GP of Prodan (Fig. 5A) it was observed that both IXH and 8-PN (tested at 100 μM) affected gel state of DPPC bilayer much more strongly than liquid-crystalline state as judged by significant flavonoid-induced reduction of GP values in temperatures below T_M (more pronounced in case of 8-PN). The experiment with the use of Laurdan revealed that IXH and 8-PN (at 100 μM) decreased DPPC main phase transition temperature (Fig. 5B). In case of this fluorescent probe no flavonoid influence on Laurdan GP values was observed in temperatures below T_M of DPPC, while slight increase of GP was induced by 8-PN in temperatures above T_M.

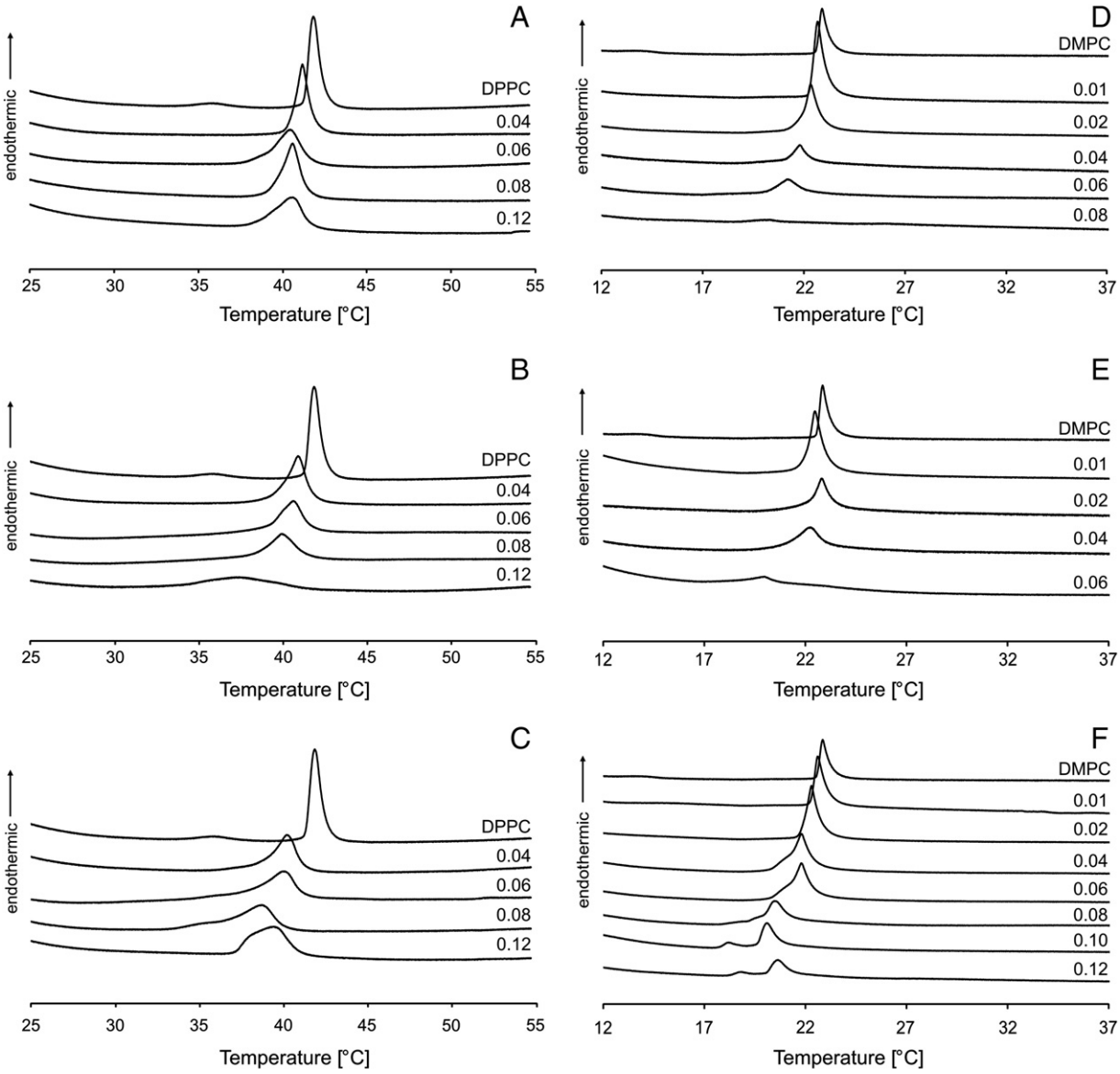

Fig. 2. The influence of prenylated polyphenols on thermotropic behavior of DPPC (left column) and DMPC (right column). The figure presents the thermograms of DPPC doped with 8-PN (A), XH (B), and IXH (C) as well as the thermograms of DMPC doped with 8-PN (D), XH (E), and IXH (F). Numbers in the figures represent polyphenol:lipid molar ratios. The thermograms were normalized to an equal amount of lipid.

Due to its sensitivity to water relaxation process, Laurdan can be also employed to detect the phase separation in lipid bilayers, i.e. the existence of lipid microdomains [21]. It is done by monitoring Laurdan generalized polarization as a function of excitation wavelength. Shortly, Laurdan GP does not depend on excitation wavelength (λ_{ex}) when bilayer is in gel state; the GP(λ_{ex}) function is increasing during phase transition or when lipid microdomains appear; and the function is decreasing when bilayer is in liquid-crystalline state. Since the results of DSC experiments suggested that IXH might induce phase separation in phosphatidylcholine model membranes, the influence of 100 μM of this compound on the dependence of Laurdan GP on excitation wavelength was studied. Fig. 6 presents GP as a function of λ_{ex} in temperatures below (Fig. 6A), near (Fig. 6B), and above DPPC phase transition (Fig. 6C). The most pronounced effect of IXH was observed at 25 °C. The GP(λ_{ex}) function became increasing in the presence of the flavonoid, while it was flat in case of pure DPPC. In higher temperatures, no IXH-induced changes of the course of GP(λ_{ex}) function were observed; only at 41 °C lower GP values were recorded in liposomes containing IXH than in pure DPPC. Similar effects were also noticed when IXH was tested at 25 μM (data not shown). On the other hand, 8-PN (tested at 100 μM) exerted no effect on the shapes of GP(λ_{ex}) functions in any of the studied temperatures (data not shown).

3.4. ATR-FTIR spectroscopy

In a frequently used approach DSC and infrared spectroscopy are applied in a parallel manner to monitor the thermal properties of biomolecules as both methods constitute sensitive tools to study the thermotropic phase behavior of lipid membranes [29] and the thermal stability of proteins [30]. In microcalorimetric experiments only cooperative changes arising from any region of lipid bilayer contribute to the measured quantity, whereas infrared data contains information resulting from both cooperative and non-cooperative phenomena. Moreover, changes locally developed in different regions of lipid bilayers can be separately analyzed by selection of appropriate probes/bands. The temperature characteristics coming from the two methods are usually discussed in terms of the intrinsic features of both techniques and the experimental conditions [31,32]. However the experimental

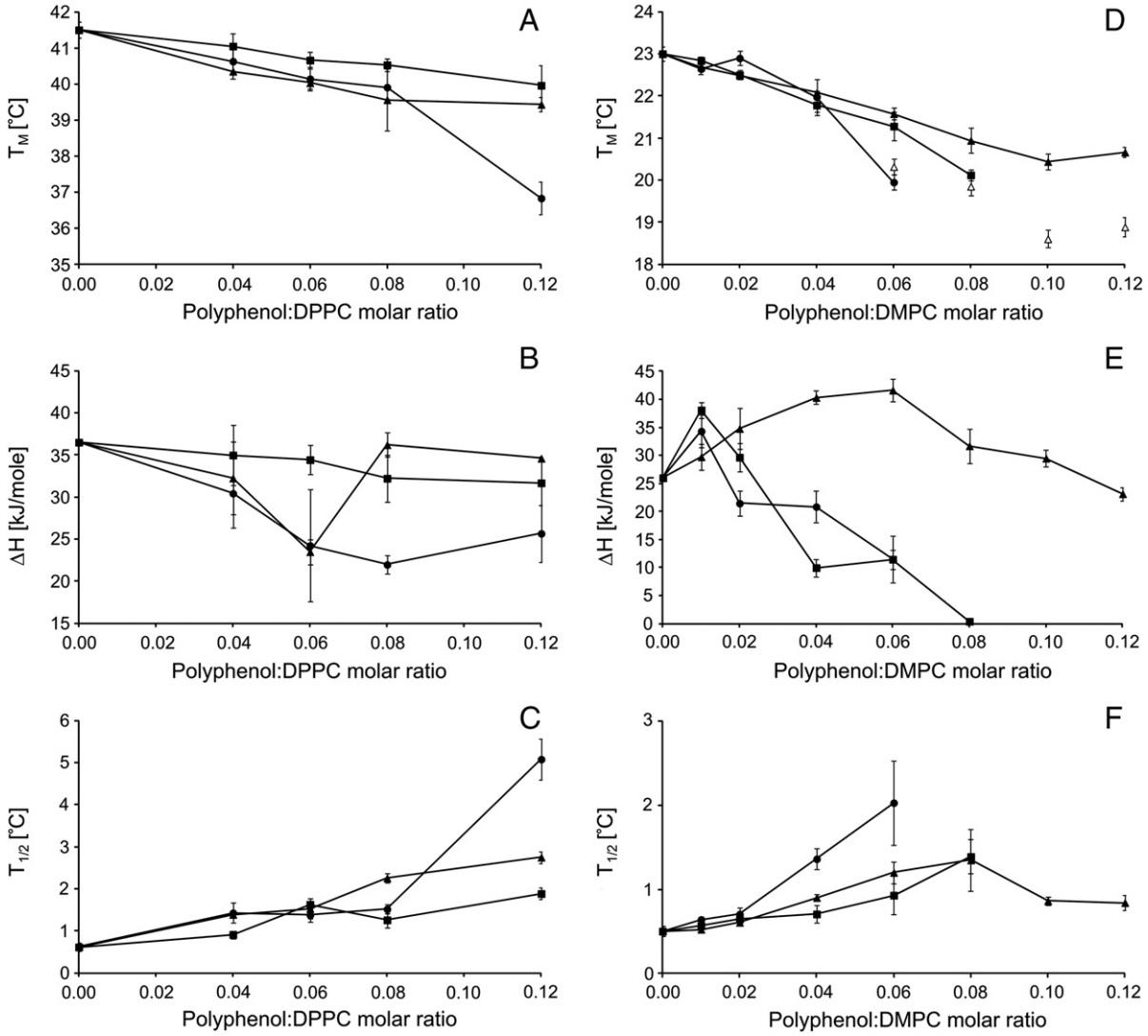

Fig. 3. Influence of 8-PN (squares), XH (circles), and IXH (triangles) on DPPC (left column) and DMPC (right column) gel–liquid crystalline phase transition parameters: temperature (A and D), enthalpy (B and E) and peak half-height width (C and F). In case of IXH:DMPC system full triangles represent maxima of the main calorimetric peak, while open triangles represent maxima of the additional peak appearing in high IXH:DMPC molar ratios (D). Bars represent standard deviations of eight measurements.

conditions have only minor influence on the differences between the values of parameters (e.g. T_M) obtained by the two methods, they have to be taken into consideration in "regional cooperativity" issue [33] based on the hypothesis that different parts of lipid molecules are subjected to nonsynchronous changes during the phase transition [34]. The "regional cooperativity" phenomenon may be examined by selection of bands behind which specific properties of different functional groups (so called probes) are hidden. Most frequently ranges composed of the νCH_2 bands and of the $\nu C{=}O$ band are selected for analysis [35,36]. First of them provides an excellent method to detect the characteristic phase transition of lipid bilayers, i.e. transition between the low temperature (gel) and the high temperature (liquid-crystalline) states accompanied by *trans-gauche* isomerization about the C – C bonds in the acyl chains. The second band is commonly used to explore the changes occurring in the interface region of a bilayer. The use of both above mentioned ranges gave us an experimental tool perfectly suited to monitor the fluidization of the lipid membrane following penetration of the studied polyphenols into its interior.

Generally, application of the principal component analysis (PCA), the most fundamental and general purpose multivariate data analysis method used in chemometrics [37,38], helps to separate total spectral changes into uncorrelated components induced by mutually orthogonal processes. In case of single principal component, PCA enables separation of the major absorbance changes induced by one process from the minor, remaining changes, which are uncorrelated with this process. Here the process of interest is the phase transition and the minor changes arise from: varying depth of penetration of the IR beam into the sample in the ATR experiment, inadequacy of the background spectrum, ineffectiveness of the pretreatment procedures, and error signal accompanying the long-standing experiment. The main merit of using PCA model, even in case of single component, is that each spectrum of a data set is treated as a whole entity defined within chosen spectral region, and all spectra are represented as linear combination of a set of representative loading values. PCA helps to extract and visualize information exclusively associated with the analyzed process. Projection of samples onto the PC1 axis gives a detailed relationship between the spectra at different stages of the phase transition process. It is called the scores plot for PC1. The obtained pattern is free of influence from the meaningless variations contained in the raw spectra. The projection of original variables onto the PC1 axis shows which of them contribute most to this pattern. It corresponds to so-called loadings plot for PC1. Such presentations are not possible in the most commonly used univariate approaches based on an arbitrary selected value from the analyzed region.

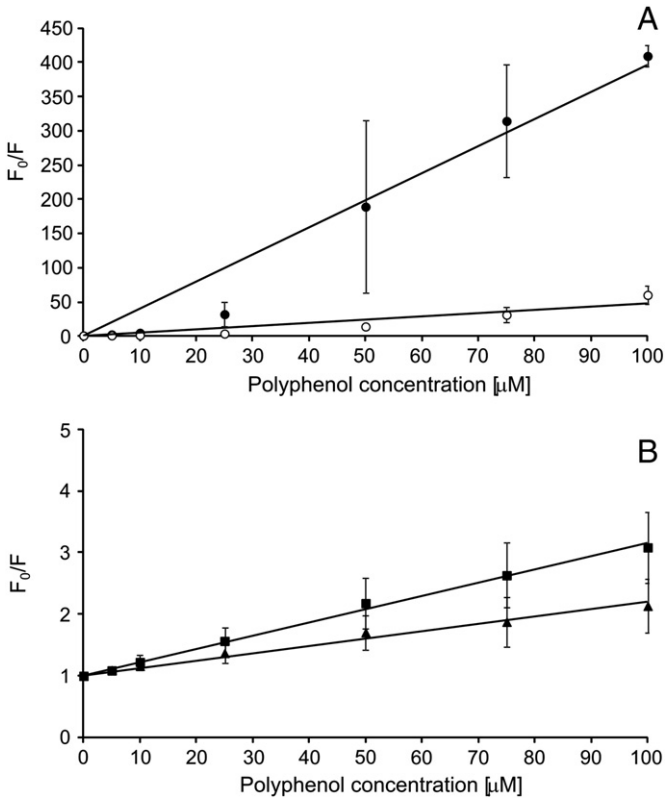

Fig. 4. Stern–Volmer plots for XH-induced quenching of Prodan (full symbols) and Laurdan (open symbols) fluorescence (A) in DPPC liposomes. Stern–Volmer plots for 8-PN (squares) and IXH-induced (triangles) quenching of Prodan fluorescence (B) in DPPC liposomes. Bars represent standard deviations of three independent experiments.

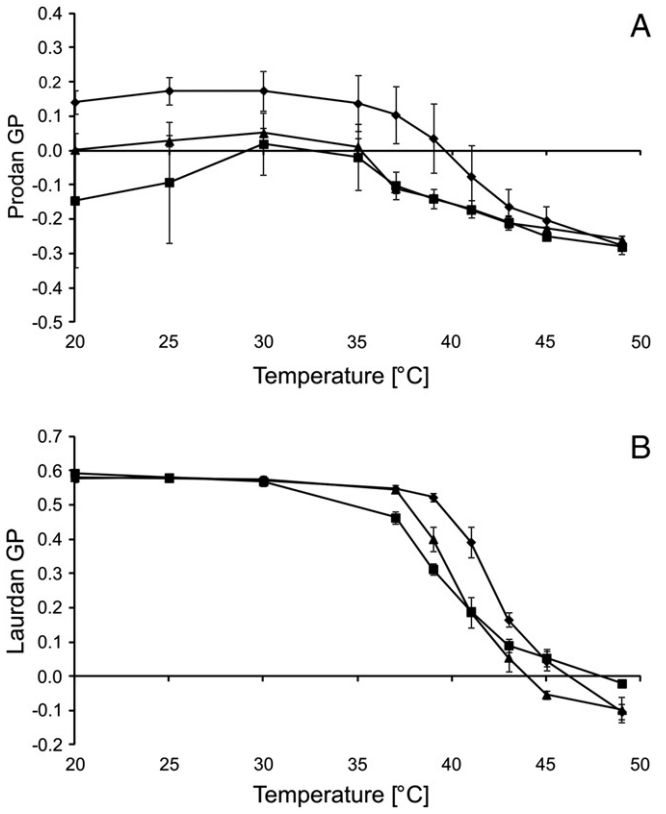

Fig. 5. Prodan (A) and Laurdan (B) generalized polarization as a function of temperature in pure DPPC liposomes (diamonds), DPPC liposomes with the addition of 100 μM 8-PN (squares), and DPPC liposomes with the addition of 100 μM IXH (triangles). Bars represent standard deviations of three independent experiments.

Fig. 7 (upper panel) presents the range from 3000 to 2800 cm^{-1} composed of bands arising from the symmetric and antisymmetric νCH_2 vibrations. For each analyzed data set the first component (PC1) described more than 98% of the temperature-induced spectral variations. It means that less than 2% of the total changes are the spectral distortions uncorrelated with the transition. The scores and loadings values for PC1 are unambiguously associated with the thermal-transition between the gel and liquid crystalline phase. Scores values plotted as a function of temperature demonstrate how the properties of the analyzed fragment of the studied system are linked to each other at subsequent stages of the heating process. The scores values (Fig. 8) fitted by a sigmoidal function (see Eq. (2)) provide two parameters describing the temperature and cooperativity of the main phase transition in the context of the local changes proceeding in the analyzed fragment of lipids. Accompanying loadings values plotted as a function of frequency (Fig. 7, lower panel) enable to detect sub-ranges of the spectral variations strictly linked with the scores values. Without the need of any initial guesses or a priori knowledge of the number and location of spectral components corresponding to the changes before and after the main transition, PCA has allowed for very accurate separation of the spectral changes captured by PC1 into two parts/sub-ranges. The spectral variations that occurred at temperatures below the main transition are sorted out by large positive loadings with maxima at 2916 and 2849 cm^{-1}. The variations that proceeded at temperatures above the transition are marked by large negative loadings which minima are at 2929 and 2857 cm^{-1}. The positions of the peaks correspond to the location of the bands assigned to the νCH_2 vibrations in the hydrocarbon chain dominated by the *trans* or *gauche* conformers.

It reveals that for pure DPPC vesicles the cooperative transition, seen by the infrared data (describing the aliphatic chain region), proceeded at the same temperature as the transition depicted by DSC data. The score runs presented in Fig. 8 for all studied systems, i.e. for DPPC and the three polyphenols, clearly show that the temperature of conversion of the predominantly ordered hydrocarbon chains to the relatively disordered liquid-crystalline state decreased in a following order: DPPC (41.50 °C) > 8-PN (40.08 °C) > IXH (39.32 °C) > XH (38.11 °C).

Fig. 9 (upper panel) shows the next analyzed range comprising changes attributed to the ester carbonyl stretching $\nu C{=}O$ band of 1,2-diacyl glycerolipids. As it has been already discussed by us [38] the shape of this band is controlled by the conformation of the diacyl chains and by intra- and intermolecular interactions in which the ester groups are involved. It can be generalized that parameters of the band are excellent probe of the hydrogen bonding interactions of the two ester groups with the residual water from the polar/apolar interfacial region [39]. Whenever analysis of the $\nu C{=}O$ band is combined with a method providing an enhancement of spectral resolution, very detailed information about interaction between the lipid esters and polar groups from a guest molecule, incorporated into the bilayer, can be gained [40]. Therefore, PCA is highly recommended for the analysis of the $\nu C{=}O$ band as the studied polyphenols were expected to exhibit different potential to penetrate into the lipid layers. It arose from the distinct number of the hydroxyl and methoxyl groups attached to the chalcone and flavonoid moieties and the different orientation of the prenyl chain with respect to them. It allowed us to presume that the studied compounds should form hydrogen bonds of different energy with the proton-acceptor C═O groups and should modify the hydration pattern in the vicinity of phospholipid ester groups.

More than 86% of total absorbance changes in this range are modeled by the first component. It means that in the $\nu C{=}O$ region the contribution from the effects uncorrelated with the main transition was larger than in the νCH_2 one. Thus, the advantage of using PCA to extract changes extremely informative for the main transition process is more pronounced in the $\nu C{=}O$ region. The loadings values plotted

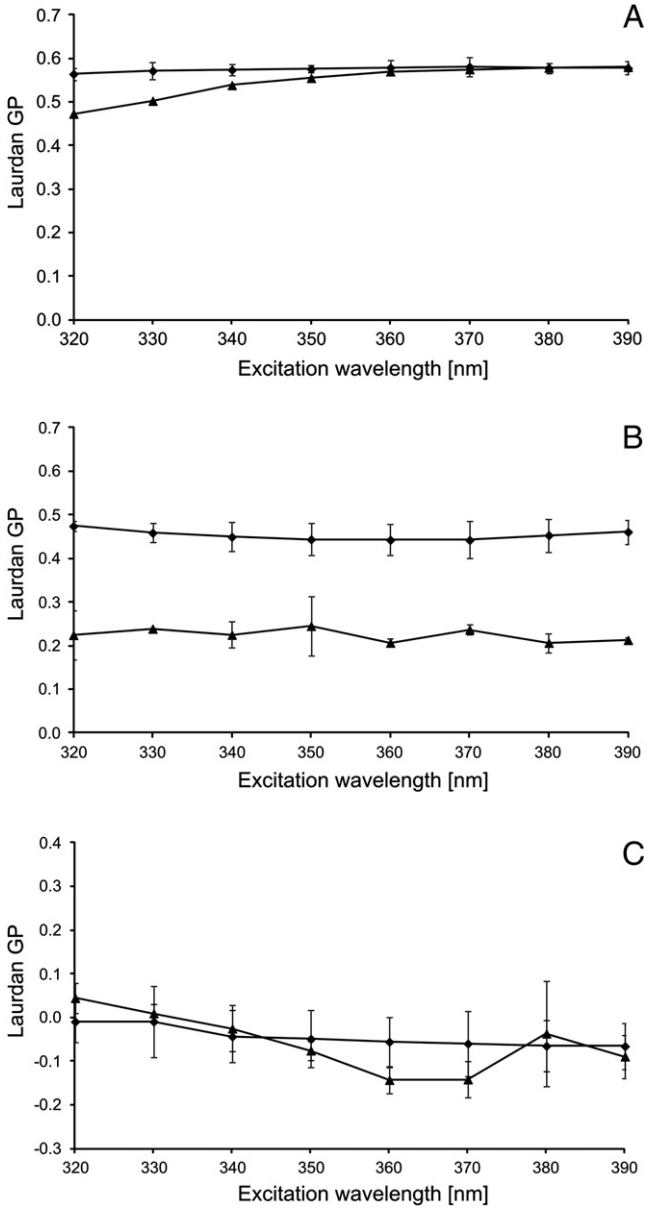

Fig. 6. Laurdan generalized polarization as a function of excitation wavelength at temperature 25 °C (A), 41 °C (B), and 49 °C (C) in pure DPPC liposomes (diamonds), and DPPC liposomes with the addition of 100 μM IXH (triangles). Bars represent standard deviations of three independent experiments.

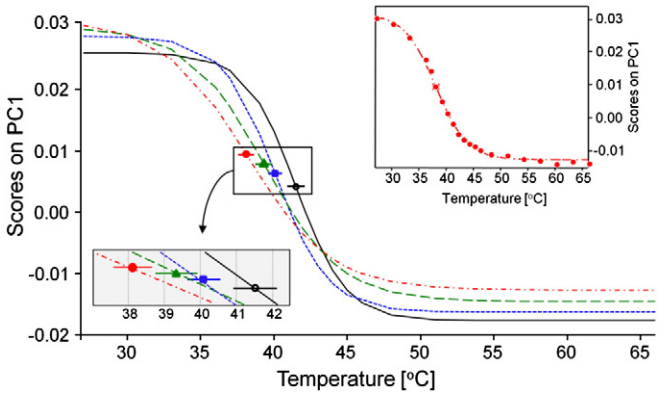

Fig. 8. The sigmoidal curves for polyphenol:DPPC mixtures at molar ratio 0.06 (DPPC — open circles, 8-PN — squares, IXH — triangles, XH — full circles) based on the PC1 scores values obtained from PCA done on the range of 3000–2800 cm^{-1}. The inset presents the sigmoidal curve together with score values for XH. For the sake of clarity the points corresponding to score values are omitted in the main figure. Black solid line — DPPC, blue dashed line — 8-PN, green dotted line — IXH, red dash-dot line — XH. The horizontal bars correspond to the standard deviation error for the T_M^{IR} value.

in the lower panel in Fig. 9 made possible to separate the spectral variations into two parts with the maximum and minimum at 1744 and 1718 cm^{-1}, respectively. The positive, high-frequency component was attributed to the νC═O vibration when the ester groups were free or weakly hydrogen bonded. According to Fig. 10 such conditions dominated at lower temperatures where the scores were positive, too. The negative, low-frequency component highlighted the changes occurring at higher temperature, i.e. those characterized by negative scores. The 26 cm^{-1} red-shift meant strengthening of the interaction of the C═O groups with water molecules and/or with hydroxyl groups from the polyphenols following the main transition. The score profiles for all studied systems that were used for the determination of the transition parameters are shown in Fig. 10. Due to the incorporation of the polyphenols into the lipid bilayer the T_M^{IR} parameters corresponding to the νC═O bands are changing in the same order as the νCH_2 band, i.e. DPPC (39.76 °C) > 8-PN (40.41 °C) > IXH (39.46 °C) > XH (38.87 °C).

4. Discussion

The influence of the studied polyphenols on the thermotropic properties of DPPC and DMPC observed by means of DSC was similar. Pretransition was completely abolished even at the lowest polyphenol: phospholipid molar ratios studied that pointed to an alteration of the lipid acyl chain packing induced by the polyphenols in the gel state [41]. The decrease of the T_M and transition cooperativity, as well as weak influence on transition enthalpy have been observed previously also for two

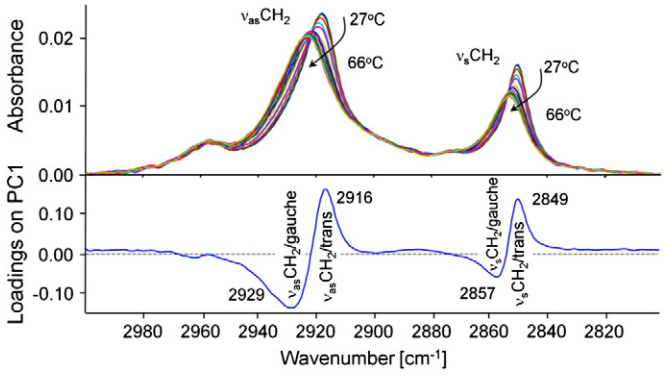

Fig. 7. Temperature-dependent absorbance changes in the range of 3000–2800 cm^{-1} (upper panel) obtained for DPPC liposome mixed with XH (at 0.06 molar ratio) and accompanying loadings plot of the first PC (lower panel).

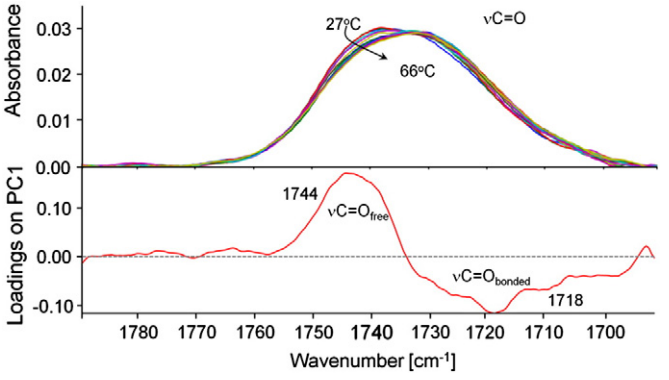

Fig. 9. Temperature-dependent absorbance changes in the range of 1790–1690 cm^{-1} (upper panel) obtained for DPPC liposome doped with XH (at 0.06 molar ratio) and associated loadings plot of the first PC (lower panel).

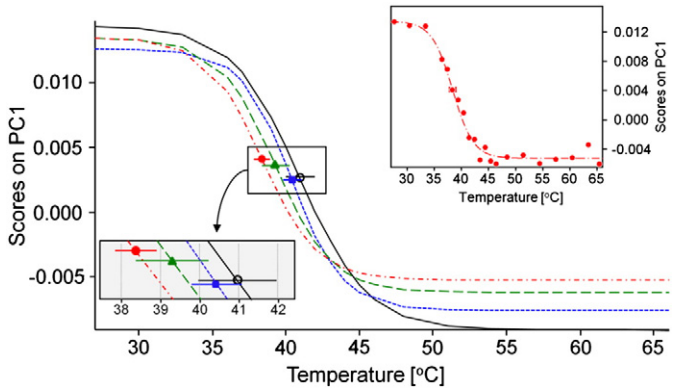

Fig. 10. The sigmoidal curves for studied polyphenol:DPPC mixtures at molar ratio 0.06 (DPPC — open circles, 8-PN — squares, IXH — triangles, XH — full circles) based on the scores PC1 values obtained from PCA done on the range of 1790–1690 cm^{-1}. The inset presents the sigmoidal curve together with score values for XH. For the sake of clarity the points corresponding to score values are omitted in the main figure. Black solid line — DPPC, blue dashed line — 8-PN, green dotted line — IXH, red dash-dot line — XH. The horizontal bars correspond to the standard deviation error for the T_M^{IR} value.

prenylated isoflavones, licoisoflavone A and 6,8-diprenylgenistein, in DPPC model membranes [42]. According to the empirical classification of DSC profiles proposed by Jain and Wu [43] such effects as observed in the present work are typical for relatively large, asymmetric, and reasonably polar dopants that affect mainly the polar–apolar interface of the membrane, partially affecting also glycerol backbone region as well as the upper part of acyl chain region of the bilayer.

Comparing the magnitude of changes induced by the studied compounds in thermotropic properties of phosphatidylcholine model membranes the order XH > IXH > 8-PN was observed. This is in accordance with the lipophilicity of polyphenol; the most lipohilic XH induced the most pronounced changes, while the least lipophilic 8-PN was the weakest membrane perturbant. The analysis of geometry-optimized structures of the studied compounds (Fig. 1) reveals that chalcone unit of XH tends to be planar, in contrast to flavonoid backbone of 8-PN and IXH. It may explain the deeper penetration of XH towards the hydrophobic region of the bilayer. Linear shape of XH molecule would also facilitate its interaction with phosphatidylcholine acyl chains. Previous studies, performed by different experimental methods, revealed that non-prenylated flavonoids might affect virtually all regions of phospholipid bilayers [44], the depth of their intercalation was, however, dependant on the flavonoid lipohilicity [44,45]. Being more lipohilic, prenylated flavonoids would intercalate even deeper into the membrane interior and alter bilayer properties to a greater extent.

The most striking feature was observed in case of phosphatidylcholine model membranes doped with IXH. In DPPC membranes significant asymmetry of the calorimetric peaks was observed in high IXH:lipid molar ratios (Fig. 2C), while in DMPC systems the new peak appeared in temperature lower than the main peak under such conditions (Fig. 2F). This may suggest the emergence of IXH-induced phase separation within a bilayer. Similar effect has been previously observed in phosphatidylcholine model membranes doped with phenothiazine derivative, trifluoperazine [26], as well as with (−)-epicatechin gallate and (−)-epigallocatechin gallate [45]. According to Jain and Wu [43] the emergence of a new peak is the result of an appearance of a new phase, modified by an additive, that coexists with the unmodified phase. Both phases differ in lipid packing characteristics and/or the size of cooperative unit. According to the authors such a behavior is expected if a dopant is localized near glycerol backbone region of the bilayer. Also Caturla et al. [45] interpreted their results for galloylated catechins in terms of the existence of additive-rich and additive-poor domains within the membrane.

It is interesting to speculate on the differences between 8-PN and IXH that may be the cause of their quite distinct effect on thermotropic properties of phosphatidylcholine model membranes observed by DSC. IXH possesses the methoxyl group in position 5 which increases its lipophilicity as compared to 8-PN (logP is 3.82 for IXH versus 1.39 for 8-PN). Moreover, an additional aromatic ring might be created by a formation of intramolecular hydrogen bond between the 5-hydroxyl group and 4-oxygen of 8-PN, as suggested previously for quercetin [46] and genistein [47]. Such a phenomenon cannot occur in case of IXH that points to different ability of the two flavonoids to interact with tightly hydrogen-bonded region of lipid polar headgroups. On the other hand, Tarahovsky et al. [48] in their theoretical paper hypothesized that relatively lipophilic flavonoids (but not chalcones) might mimic the action of cholesterol in membranes and favor the formation of microdomains in lipid model membranes.

Fluorescent probes, Prodan and Laurdan, constitute useful tools to monitor phospholipid phase transitions since spectral properties of both probes depend strongly on the amount of water penetrating the appropriate regions of a bilayer (hydrophobic–hydrophilic interface in case of Laurdan, and polar headgroup region in case of Prodan) as well as on the dynamics of water molecules, especially on the amount of the solvent dipolar relaxation process occurring in the vicinity of the fluorescent label [28]. Since gel and liquid-crystalline states of a bilayer differ not only in lipid order but also in hydration and water molecules' dynamics, the main phospholipid phase transition manifests itself in a sharp drop of Laurdan or Prodan GP values (from positive values in gel state to negative ones in liquid-crystalline state). The results obtained in the present work show that both 8-PN and IXH decrease melting temperature of DPPC bilayers which is in accordance with microcalorimetric results. The influence of the flavonoids was noticeable in membrane regions monitored both by Prodan and Laurdan. The flavonoid-induced reduction in Prodan GP values observed in temperatures below T_M suggests that the flavonoids affected DPPC headgroup packing and hydration in such a way that more water molecules were able to incorporate at the hydrophobic—hydrophilic interface of model membrane in gel state. An alternative explanation of this observation may also be the reduction of Prodan partitioning into DPPC bilayer in gel state caused by the addition of 8-PN and IXH. Prodan exhibits significant fluorescence in water [49] and its emission spectrum is strongly red-shifted in this solvent. Therefore the presence of excess Prodan molecules in buffer medium of the studied system would also result in the decrease of the observed GP values.

Additionally, the experiments in which the course of Laurdan GP(λ_{ex}) function was analyzed showed that IXH, but not 8-PN, was able to induce lipid phase separation in DPPC bilayers in temperatures below T_M. That is again in accordance with DSC results. This observation may be explained by the appearance of IXH-rich and IXH-poor microdomains within a bilayer that may differ in hydration and lipid packing. However, the precise determination of the nature of IXH-induced lipid domains would require further studies.

In our studies IXH and 8-PN turned out to be very weak quenchers of Prodan, but not Laurdan, fluorescence. In contrast, XH strongly quenched fluorescence of both probes. The decreased fluorescence intensity in the presence of the polyphenols may be the result of their interaction with fluorescent probes affecting e.g. their molecular organization within the bilayer or their influence on fluorophores' microenvironment. The more pronounced quenching of Prodan than that of Laurdan fluorescence exhibited by all the studied compounds indicates that the bilayer region occupied by Prodan is more affected by the presence of the polyphenols. Flavonoids from different subclasses as well as chalcones have been previously observed to quench the fluorescence of some fluorescent probes [50,51]. Schoefer et al. recorded the weaker ability of flavanones, as compared to chalcones, to quench DPH fluorescence [50]. They attributed it to the difference in their structure — chalcones possess, instead of ring C, one double bond and one oxo group that together form the π-conjugated system throughout the whole molecule, while the lack of the double bond in ring C of flavanones restricts the size of conjugated double bond system within their molecules.

For the pure DPPC vesicles there is a perfect agreement between the phase transition temperatures determined by DSC (41.50 °C ± 0.22) and obtained from the analysis of the νCH_2 absorption bands (41.50 °C ± 0.28). It points to the fact that effects depicted by the two methods arise from changes in interactions between hydrocarbon chains in gel phase that are much stronger than in fluid phase. In case of the pure DPPC sample, the T_M^{IR} value recorded for the $\nu C{=}O$ probe is lower from the T_M value obtained by means of DSC. The lower T_M^{IR} value obtained from the $\nu C{=}O$ band means that the changes in hydration of the polar–apolar interfacial part proceeded earlier, i.e. at lower temperature than those in the region of the hydrocarbon chains. In other words, it reveals that the changes realized in the region of the hydrophobic chains are initiated by those developed in the polar—apolar part due to its smaller thermal stability caused by the perturbing interactions with water molecules.

Fig. 11 summarizes the infrared spectroscopy results showing that partitioning of 8-PN, IXH, and XH molecules caused different fluidization of the DPPC bilayers. A small logP value for 8-PN (1.39) in relation to other two polyphenols may explain its weak effect on the thermotropic properties of DPPC membrane. When comparing the temperatures for 8-PN obtained from the two spectral ranges it can be stated that this flavanone first disturbed the lateral packing interactions between hydrocarbon chains and at slightly higher temperature the changes in the polar—apolar interface proceeded. It can be expected that the hydrogen bonding interaction between the three hydroxyl groups of 8-PN and the ester groups of lipid is responsible for the different order of the changes as compared to that observed in pure DPPC. Additionally, the interactions between the ether and ketone oxygens and water molecules occupying the polar—apolar region change electrostatic properties in this part of 8-PN-doped DPPC bilayer. After 8-PN incorporation into the network of hydrogen bonds formed by the lipid and water molecules the polar—apolar region of a bilayer became relatively more stable than the hydrophobic region disturbed by the presence of the prenyl chains.

In case of IXH the methoxyl group in position 5 increases its lipophilic character — as it is proved by logP increase to 3.82, as compared to 1.39 for 8-PN. In a consequence IXH molecules may penetrate more deeply into the interfacial region. Moreover, due to the larger steric, unpolar hindrance in case of IXH there are larger changes in packing in the polar–apolar interface. The polar–apolar region is no longer more stable from the apolar one, as it was for 8-PN:DPPC system.

According to ATR-FTIR results, XH affected the properties of DPPC model membranes most strongly that cannot be totally attributed to its high lipophilicity (logP = 4.38). The deeper penetration of XH into the lipid interior can be explained when configuration of the chalcone unit is compared with that for flavanone. In case of XH the larger planarity of the unit facilitates deeper penetration of the prenyl chain into the lipid layers. A and B rings of 8-PN and IXH are oriented at angle of 76.5° and 69.9°, respectively, and therefore the molecules have an elbow shape. For XH the two rings have more planar orientation (21.2° — the calculated, and 3.1° — the X-ray determined value) and due to the interaction with the oriented DPPC molecules could adopt a linear shape that guarantied its better diffusion into the lipid layers.

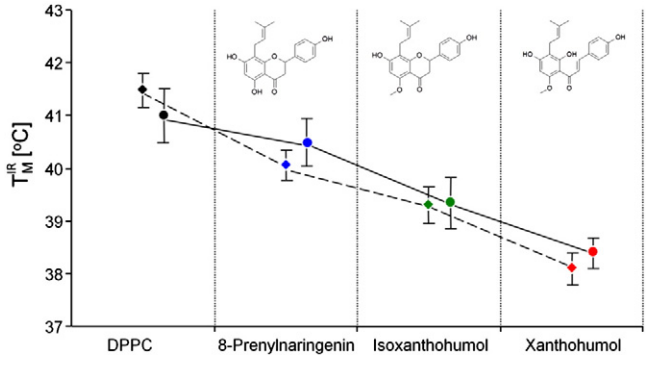

Fig. 11. The T_M^{IR} values obtained on the basis of PCA applied to the ATR-FTIR spectra for the range of 3000–2800 cm^{-1} (diamonds) characteristic for absorbance arising from the νCH_2 stretching bands and for the range of 1790–1690 cm^{-1} (circles) dominated by the $\nu C{=}O$ stretching band. Bars represent the standard deviation error.

Our results obtained for fully hydrated systems are contradictory to the ones obtained for the dry film by Arczewska et al. [20]. These authors postulated the weakening of the interaction of XH with hydrocarbon chains during heating process resulting in the removal of XH from the interfacial parts of lipid bilayer. It was proposed that long axes of XH molecules were orientated perpendicularly to the bilayer normal. Our ATR-FTIR results clearly show that XH penetrates more deeply into the bilayer interior than 8-PN and IXH. The differences in penetration are well explained when XH is considered as a rod-shape molecule whose long axis is oriented parallel to the normal of the membrane, while 8-PN and IXH due to their elbow shape are locked at the polar–apolar region and only their prenyl chains incorporate into the hydrophobic part of the bilayer.

The most important source of XH and related compounds in human diet is beer. Although XH prevails in hops, main prenylated flavonoid in beer is IXH formed from XH during the brewing process [1]. Average daily intake of these compounds is estimated to be c.a. 0.14 mg [1]. The data on their bioavailability are rather scarce in the literature, however the absorption of polyphenols in the small intestine is believed to be rather low (10–20%) [52]. On the other hand, c.a. 10-fold increase of 8-PN concentration was reported to be achievable in the colon due to the activity of its microbial community [52]. The studies in rats fed with XH [53] and women orally administered with hop supplements [54] revealed plasma concentrations of prenylflavonoids to range from a few nM [54] to a few μM [53]. However, cell culture studies showed that Caco-2 intestinal epithelial cells and hepatocytes [55] could accumulate XH present in medium, resulting in intracellular concentration of XH being c.a. 60 times higher than the extracellular one.

The concentrations of hop polyphenols used in the present model study were much higher than the ones reported to be physiologically achievable. This is the common disadvantage of model studies in which the necessity of using of high additive concentrations comes mainly from technical reasons. In spite of being far from the real membranes, one-component lipid systems constitute the basic essential step in understanding the interaction of XH, IXH and 8-PN with biomembranes. However, as stated above, high local concentrations of an additive might be achieved when it enters cellular system. Therefore, such a model study clearly constitutes an important step in understanding polyphenol–membrane interaction scheme. It is, anyway, obvious that an extreme caution is needed when transferring the findings from model systems into in vivo situation.

5. Conclusions

The results of experiments performed by means of DSC, fluorescence spectroscopy and ATR-FTIR spectroscopy clearly demonstrate that three prenylated polyphenols from common hop, flavanones 8-PN and IXH, and chalcone XH strongly affect biophysical properties of DPPC model membranes. The presence of the polyphenols alters the parameters describing main phospholipid phase transition, as well as lipid order and hydration of membrane. All the studied compounds intercalate into lipid bilayer, influencing its glycerol backbone region, hydrocarbon chain region, and, to a lesser extent, polar head group region. The magnitude of effects exerted by the studied polyphenols on DPPC membranes is positively correlated with their lipophilicity. The precise localization of the polyphenols in DPPC bilayer depends also on their molecular shape. An additional, striking feature noticed in the present study was the ability of IXH to induce lateral lipid phase separation in phospatidylcholine bilayers. The results have been interpreted with the assumption that IXH-rich and IXH-poor microdomains appeared

within the membrane, however the precise determination of the nature of these putative domains would require further studies.

Supplementary data to this article can be found online at http://dx.doi.org/10.1016/j.bbamem.2013.09.009.

Acknowledgments

This work was financed by Polish Ministry of Science and Higher Education funds for Wroclaw Medical University and by grant no. N N204 150440 (for J.P.). The authors acknowledge the *Wroclaw Centre for Networking and Supercomputing* (http://www.wcss.wroc.pl) for the generous access to computer time.

References

[1] J.F. Stevens, J.E. Page, Xanthohumol and related prenylflavonoids from hops and beer: to your good health! Phytochemistry 65 (2004) 1317–1330.
[2] S. Milligan, J. Kalita, V. Pocock, A. Heyerick, L. De Cooman, H. Rong, D. De Keukeleire, Oestrogenic activity of the hop phyto-oestrogen, 8-prenylnaringenin, Reproduction 123 (2002) 235–242.
[3] R. Monteiro, H. Becker, I. Azevedo, C. Calhau, Effect of hop (*Humulus lupulus* L.) flavonoids on aromatase (estrogen synthase) activity, J. Agric. Food Chem. 54 (2006) 2938–2943.
[4] M.S. Pepper, S.J. Hazel, M. Humpel, W.D. Schleuningm, 8-prenylnaringenin, a novel phytoestrogen, inhibits angiogenesis *in vitro* and *in vivo*, J. Cell. Physiol. 199 (2004) 98–107.
[5] T. Paoletti, S. Fallarini, F. Gugliesi, A. Minassi, G. Appendino, G. Lombardi, Anti-inflammatory and vascularprotective properties of 8-prenylapigenin, Eur. J. Pharmacol. 620 (2009) 120–130.
[6] C. Di Vito, A. Bertoni, M. Nalin, S. Sampietro, M. Zanfa, F. Sinigaglia, The phytoestrogen 8-prenylnaringenin inhibits agonist-dependent activation of human platelets, Biochim. Biophys. Acta 1820 (2012) 1724–1733.
[7] M.R. Peluso, C.L. Miranda, D.J. Hobbs, R.R. Proteau, J.F. Stevens, Xanthohumol and related prenylated flavonoids inhibit inflammatory cytokine production in LPS-activated THP-1 monocytes: structure–activity relationships and in silico binding to myeloid differentiation protein-2 (MD-2), Planta Med. 76 (2010) 1536–1543.
[8] C. Gerhauser, Broad spectrum anti-infective potential of xanthohumol from hop (*Humulus lupulus* L.) in comparison with activities of other hop constituents and xanthohumol metabolites, Mol. Nutr. Food Res. 49 (2005) 827–831.
[9] S.H. Lee, H.J. Kim, J.S. Lee, I.S. Lee, B.Y. Kang, Inhibition of topoisomerase I activity and efflux drug transporters' expression by xanthohumol from hops, Arch. Pharm. Res. 30 (2007) 1435–1439.
[10] C.L. Miranda, J.F. Stevens, A. Helmrich, M.C. Henderson, R.J. Rodriguez, Y.H. Yang, M.L. Deinzer, D.W. Barnes, D.R. Buhler, Antiproliferative and cytotoxic effects of prenylated flavonoids from hops (*Humulus lupulus*) in human cancer cell lines, Food Chem. Toxicol. 37 (1999) 271–285.
[11] E. Brunelli, A. Minassi, G. Appendino, L. Moro, 8-Prenylnaringenin, inhibits estrogen receptor-a mediated cell growth and induces apoptosis in MCF-7 breast cancer cells, J. Steroid Biochem. Mol. Biol. 107 (2007) 140–148.
[12] L. Delmulle, A. Bellahcene, W. Dhooge, F. Comhaire, F. Roelens, K. Huvaere, A. Heyerick, V. Castronovo, D. De Keukeleire, Anti-proliferative properties of prenylated flavonoids from hops (*Humulus lupulus* L.) in human prostate cancer cell lines, Phytomedicine 13 (2006) 732–734.
[13] E.C. Colgate, C.L. Miranda, J.F. Stevens, T.M. Bray, E. Ho, Xanthohumol, a prenylflavonoid derived from hops induces apoptosis and inhibits NF-kappaB activation in prostate epithelial cells, Cancer Lett. 246 (2007) 201–209.
[14] D. Deeb, X. Gao, H. Jiang, A.S. Arbab, S.A. Dulchavsky, S.C. Gautam, Growth inhibitory and apoptosis-inducing effects of xanthohumol, a prenylated chalone present in hops, in human prostate cancer cells, Anticancer. Res. 30 (2010) 3333–3339.
[15] R. Benelli, R. Vene, M. Ciarlo, S. Carlone, O. Barbieri, N. Ferrari, The AKT/NF-κB inhibitor xanthohumol is a potent anti-lymphocytic leukemia drug overcoming chemoresistance and cell infiltration, Biochem. Pharmacol. 83 (2012) 1634–1642.
[16] O. Wesolowska, J. Wisniewski, K. Sroda, A. Krawczenko, A. Bielawska-Pohl, M. Paprocka, D. Dus, K. Michalak, 8-Prenylnaringenin is an inhibitor of multidrug resistance-associated transporters, P-glycoprotein and MRP1, Eur. J. Pharmacol. 644 (2010) 32–40.
[17] C.L. Miranda, J.F. Stevens, V. Ivanov, M. McCall, B. Frei, M.L. Deinzer, D.R. Buhler, Antioxidant and prooxidant actions of prenylated and nonprenylated chalcones and flavanones *in vitro*, J. Agric. Food Chem. 48 (2000) 3876–3884.
[18] J.F. Stevens, C.L. Miranda, B. Frei, D.R. Buhler, Inhibition of peroxynitrite-mediated LDL oxidation by prenylated flavonoids: the alpha, beta-unsaturated keto functionality of 2′-hydroxychalcones as a novel antioxidant pharmacophore, Chem. Res. Toxicol. 16 (2003) 1277–1286.
[19] R.J. Rodriguez, C.L. Miranda, J.F. Stevens, M.L. Deinzer, D.R. Buhler, Influence of prenylated and non-prenylated flavonoids on liver microsomal lipid peroxidation and oxidative injury in rat hepatocytes, Food Chem. Toxicol. 39 (2001) 437–445.
[20] M. Arczewska, D.M. Kaminski, E. Gorecka, D. Pociecha, E. Roj, A. Slawinska-Brych, M. Gagos, The molecular organization of prenylated flavonoid xanthohumol in DPPC multibilayers: X-ray diffraction and FTIR spectroscopic studies, Biochim. Biophys. Acta 1828 (2013) 213–222.
[21] T. Parasassi, G. De Stasio, A. dUbaldo, E. Gratton, Phase fluctuation in phospholipid membranes revealed by Laurdan fluorescence, Biophys. J. 57 (1990) 1179–1186.
[22] M.J. Frisch, G.W. Trucks, H.B. Schlegel, G.E. Scuseria, M.A. Robb, J.R. Cheeseman, G. Scalmani, V. Barone, B. Mennucci, G.A. Petersson, H. Nakatsuji, M. Caricato, X. Li, H.P. Hratchian, A.F. Izmaylov, J. Bloino, G. Zheng, J.L. Sonnenberg, M. Hada, M. Ehara, K. Toyota, R. Fukuda, J. Hasegawa, M. Ishida, T. Nakajima, Y. Honda, O. Kitao, H. Nakai, T. Vreven, J.A. Montgomery Jr., J.E. Peralta, F. Ogliaro, M. Bearpark, J.J. Heyd, E. Brothers, K.N. Kudin, V.N. Staroverov, R. Kobayashi, J. Normand, K. Raghavachari, A. Rendell, J.C. Burant, S.S. Iyengar, J. Tomasi, M. Cossi, N. Rega, J.M. Millam, M. Klene, J.E. Knox, J.B. Cross, V. Bakken, C. Adamo, J. Jaramillo, R. Gomperts, R.E. Stratmann, O. Yazyev, A.J. Austin, R. Cammi, C. Pomelli, J.W. Ochterski, R.L. Martin, K. Morokuma, V.G. Zakrzewski, G.A. Voth, P. Salvador, J.J. Dannenberg, S. Dapprich, A.D. Daniels, O. Farkas, J.B. Foresman, J.V. Ortiz, J. Cioslowski, D.J. Fox, Gaussian 09, Revision B.01, Gaussian Inc., Wallingford, CT, 2009.
[23] L.R. Chadwick, D. Nikolic, J.E. Burdette, C.R. Overk, J.L. Bolton, R.B. van Breemen, R. Fröhlich, H.H.S. Fong, N.R. Farnsworth, G.F. Pauli, Estrogens and congeners from spent hops (*Humulus lupulus*), J. Nat. Prod. 67 (2004) 2024–2032.
[24] F.H. Allen, The Cambridge Structural Database: a quarter of a million crystal structures and rising, Acta Crystallogr. B Struct. Sci. 58 (2002) 380–388.
[25] I.V. Tetko, J. Gasteiger, R. Todeschini, A. Mauri, D. Livingstone, P. Ertl, V.A. Palyulin, E.V. Radchenko, N.S. Zefirov, A.S. Makarenko, V.Y. Tanchuk, V.V. Prokopenko, Virtual computational chemistry laboratory — design and description, J. Comput. Aided Mol. Des. 19 (2005) 453–463.
[26] A.B. Hendrich, O. Wesolowska, K. Michalak, Trifluoperazine induces domain formation in zwitterionic phosphatidylcholine but not in charged phosphatidylglycerol bilayers, Biochim. Biophys. Acta 1510 (2001) 414–425.
[27] E. Theodoropoulou, D. Marsh, Interactions of angiotensin II non-peptide AT1 antagonist losartan with phospholipid membranes studied by combined use of differential scanning calorimetry and electron spin resonance spectroscopy, Biochim. Biophys. Acta 1461 (1999) 135–146.
[28] T. Parasassi, E.K. Krasnowska, L. Bagatolli, E. Gratton, Laurdan and Prodan as polarity-sensitive fluorescent membrane probes, J. Fluoresc. 8 (1998) 365–373.
[29] Y.P. Zhang, R.N.A.H. Lewis, R.N. McElhaney, Calorimetric and spectroscopic studies of the thermotropic phase behavior of the n-saturated 1,2-diacylphosphatidylglycerols, Biophys. J. 72 (1997) 779–793.
[30] A.I. Azuaga, F. Sepulcre, E. Padros, P.L. Mateo, Scanning calorimetry and Fourier-transform infrared studies into the thermal stability of cleaved bacteriorhodopsin systems, Biochemistry 35 (1996) 16328–16335.
[31] E. Mueller, A. Giehl, G. Schwarzmann, K. Sandhoff, A. Blume, Oriented 1,2-dimyristoyl-sn-glycero-3-phosphorylcholine/ganglioside membranes: a Fourier transform infrared attenuated total reflection spectroscopic study. Band assignments; orientational, hydrational, and phase behavior; and effects of Ca^{2+} binding, Biophys. J. 71 (1996) 1400–1421.
[32] R. Chehin, I. Iloro, M.J. Marcos, E. Villar, V.L. Shnyrov, J.L. Arrondo, Thermal and pH-induced conformational changes of a beta-sheet protein monitored by infrared spectroscopy, Biochemistry 38 (1999) 1525–1530.
[33] F.G. Wu, Q. Jia, R.G. Wu, Z.W. Yu, Regional cooperativity in the phase transitions of dipalmitoylphosphatidylcholine bilayers: the lipid tail triggers the isothermal crystallization process, J. Phys. Chem. B 115 (2011) 8559–8568.
[34] F.G. Wu, N.N. Wang, J.S. Yu, J.J. Luo, Z.W. Yu, Nonsynchronicity phenomenon observed during the lamellar–micellar phase transitions of 1-stearoyllysophosphatidylcholine dispersed in water, J. Phys. Chem. B 114 (2010) 2158–2164.
[35] R. Mendelsohn, IR spectroscopy of lipid chains: theoretical background and applications to phase transitions, membranes, cells and tissues, in: P.L. Yeagle (Ed.), The Structure of Biological Membranes, 3rd edition, CRC Press, Boca Raton, 2012, pp. 91–118.
[36] R.N.A.H. Lewis, R.N. McElhaney, Review: membrane lipid phase transitions and phase organization studied by Fourier transform infrared spectroscopy, Biochim. Biophys. Acta (2012), http://dx.doi.org/10.1016/j.bbamem.2012.10.018.
[37] K.H. Esbensen, P. Geladi, Principal component analysis: concept, geometrical interpretation, mathematical background, algorithms, history, practice, in: S.D. Brown, R. Tauler, B. Walczak (Eds.), Comprehensive Chemometrics Chemical and Biochemical Data Analysis, vol. 2, Elsevier Science, 2009, pp. 211–226.
[38] J. Petrus, B. Czarnik-Matusewicz, Investigation of the polarization dependent attenuated total reflection infrared spectra of ordered lipids assisted by principal component analysis, Vib. Spectrosc. 62 (2012) 133–142.
[39] A. Blume, W. Hubner, G. Messner, Fourier transform infrared spectroscopy of $^{13}C{=}O$ labelled phospholipids hydrogen bonding to carbonyl groups, Biochemistry 27 (1988) 8239–8249.
[40] J. Szwed, K. Cieslik-Boczula, B. Czarnik-Matusewicz, A. Jaszczyszyn, K. Gasiorowski, P. Swiątek, W. Malinka, Moving-window 2D correlation spectroscopy in studies of fluphenazine–DPPC dehydrated film as a function of temperature, J. Mol. Struct. 974 (2010) 192–202.
[41] T. Heimburg, A model for the lipid pretransition:coupling of ripple formation with the chain-melting transition, Biophys. J. 78 (2000) 1154–1165.
[42] A.B. Hendrich, R. Malon, A. Pola, Y. Shirataki, N. Motohashi, K. Michalak, Differential interaction of *Sophora* isoflavonoids with lipid bilayers, Eur. J. Pharm. Sci. 16 (2002) 201–208.
[43] M.K. Jain, N.M. Wu, Effects of small molecules on the dipalmitoyl lecithin liposomal bilayer. III. Phase transitions of lipid bilayers, J. Membr. Biol. 34 (1977) 157–201.
[44] H.A. Scheidt, A. Pampel, L. Nissler, R. Gebhardt, D. Huster, Investigation of the membrane localization and distribution of flavonoids by high-resolution magic angle spinning NMR spectroscopy, Biochim. Biophys. Acta 1663 (2004) 97–107.
[45] N. Caturla, E. Vera-Samper, J. Villalain, C.R. Mateo, V. Micol, The relationship between the antioxidant and the antibacterial properties of galloylated catechins and the structure of phospholipid model membranes, Free Radic. Biol. Med. 34 (2003) 648–662.
[46] L. Movileanu, I. Neagoe, M.L. Flonta, Interaction of the antioxidant flavonoid quercetin with planar lipid bilayers, Int. J. Pharm. 205 (2000) 135–146.

[47] R. Kato, K. Kajiya, H. Tokumoto, S. Kumazawa, T. Nakayama, Affinity of isoflavonoids for lipid bilayers evaluated with liposomal systems, Biofactors 19 (2003) 179–187.
[48] Y.S. Tarahovsky, E.N. Muzafarov, Y.A. Kim, Rafts making and rafts braking: how plant flavonoids may control membrane heterogeneity, Mol. Cell. Biochem. 314 (2008) 65–71.
[49] E.K. Krasnowska, E. Gratton, T. Parasassi, Prodan as a membrane surface fluorescence probe: partitioning between water and phospholipid phases, Biophys. J. 74 (1998) 1984–1993.
[50] L. Schoefer, A. Braune, M. Blaut, A fluorescence quenching test for the detection of flavonoid transformation, FEMS Microbiol. Lett. 204 (2001) 277–280.
[51] O. Wesolowska, A.B. Hendrich, B. Lania-Pietrzak, J. Wisniewski, J. Molnar, I. Ocsovszki, K. Michalak, Perturbation of lipid phase of membrane is not involved in modulation of MRP1 transport activity by flavonoids, Cell. Mol. Biol. Lett. 14 (2009) 199–221.
[52] S. Possemiers, A. Heyerick, V. Robbens, D. De Keukeleire, W. Verstraete, Activation of proestrogens from hops (*Humulus lupulus* L.) by intestinal microbiota; conversion of isoxanthohumol into 8-prenylnaringenin, J. Agric. Food Chem. 53 (2005) 6281–6288.
[53] L. Hanske, G. Loh, S. Sczesny, M. Blaut, A. Braune, Recovery and metabolism of xanthohumol in germ-free and human microbiota-associated rats, Mol. Nutr. Food Res. 54 (2010) 1405–1413.
[54] S. Bolca, J. Li, D. Nikolic, N. Roche, P. Blondeel, S. Possemiers, D. De Keukeleire, M. Bracke, A. Heyerick, R.B. van Breemen, H. Depypere, Disposition of hop prenylflavonoids in human breast tissue, Mol. Nutr. Food Res. 54 (2010) S284–S294.
[55] H. Wolff, M. Motyl, C. Hellerbrand, J. Heilmann, B. Kraus, Xanthohumol uptake and intracellular kinetics in hepatocytes, hepatic stellate cells, and intestinal cells, J. Agric. Food Chem. 59 (2011) 12893–12901.